

Numerical Investigation of Wave Interaction with Horizontal Plate Breakwaters by Coupled CFD-FEM Method

Jiawei Xiao¹, Guohua Pan², Jianhua Wang¹, Decheng Wan^{1*}

¹ Computational Marine Hydrodynamics Lab (CMHL), School of Naval Architecture, Ocean and Civil Engineering, Shanghai Jiao Tong University, Shanghai, China

² Ningbo Pilot Station, Ningbo Dagang Pilotage Co., Ltd., Ningbo, China

*Corresponding Author

ABSTRACT

In this paper, a two-way coupled CFD-FEM (Computational Fluid Dynamics and Finite Element Method) program is applied to numerically simulate wave interaction with horizontal plate breakwaters. The method of CFD-FEM is constructed based on preCICE, which is an open-source coupling library for partitioned multi-physics simulations. The flow field is solved by RANS method with OpenFOAM and the structural part is solved by FEM with Calculix. The results of the numerical simulations are compared with the existing literature results, and the results of the elastic thin structure are in good agreement of the literature results. The maximum error of reflection coefficient K_r is 10.3%, the maximum error of transmission coefficient K_t is 6.6%, and the maximum error of RAO of the deformation δ_z at point A is 9.7%. The results of elastic and rigid horizontal plate breakwaters are compared to better understand the effects of the structure deformation on the hydrodynamics.

KEY WORDS: wave interaction, CFD-FEM, overset, horizontal plate breakwaters.

INTRODUCTION

Breakwaters have an important role in port facilities. Conventional breakwaters are generally bottom breakwaters. Currently open breakwaters such as horizontal plate breakwaters (HPB) have received more attention. Heins (1950) carried out pioneering work on rigid horizontal plate breakwaters (RHPB). His work derived explicit formulas for the reflection and transmission coefficients of a semi-infinite width rigid plate submerged in a finite water depth using the Wiener-Hopf technique. Since then, a number of theoretical, numerical and experimental studies have been carried out to better understand the hydrodynamic properties of the structure. (Greene and Heins (1953), Ijima et al (1970), Brossard et al (2009), Qi and Hou(2003))

A study by I. Cho and M. Kim (1999) suggested that resilient breakwaters may have better wave shielding performance compared to

rigid breakwaters. For research purposes, an elastic horizontal plate breakwater (EHPB) can be modelled as an elastic thin plate. Lee and Chen (2010) proposed a linear analytical solution to the wave interaction problem for an articulated elastic vertical plate breakwater. Based on this theoretical solution, the effect of structural flexibility on reflected and transmitted waves was investigated. Ashok et al (2020) presented an analytical solution for wave scattering from porous flexible vertical elastic plates and tensioned membranes where the reflection and transmission coefficients are explicitly represented. In the above work, the interaction of waves with elastic breakwaters was investigated using potential flow theory. However, the potential flow theory can only deal with inviscid fluids without considering viscosity. This may lead to inaccuracies when solving specific engineering problems characterized by wave breaking.

Due to the advances in Computational Fluid Dynamics (CFD), several viscous flow models based on the Navier-Stokes equations for solving fluid phases have been developed. In general, CFD methods can be categorized into mesh-based and meshless methods. Among the mesh-based methods, FDM and finite volume method (FVM) are the most common methods for this particular topic. Liao and Hu (2013) developed a fluid-solid coupling (FSI) model to simulate tank swaying with elastic cantilever walls. In this model, the fluid and solid phases were solved by finite difference and finite element methods, respectively, and coupled by a conservative momentum exchange method based on the submerged boundary method. Hu et al. (2023) combined the IHFOAM wave modelling toolkit based on FVM with the fully-coupled FSI method to study the hydroelasticity of a vertical wall subjected to waves elasticity, aiming at a comprehensive understanding of the nonlinear wave evolution and the corresponding structural response. Attili et al (2023) simulated the wave impact on a flexible plate by means of the open-source FVM toolbox Solids4FOAM (Cardiff (2018)), implemented in OpenFOAM, and validated the model by means of an ad hoc experiment. Lagrangian meshfree methods (particle methods) can also be applied in related studies. Khayyer et al (2021) combined the incompressible SPH (ISPH) model of the fluid phase with the Hamiltonian SPH model of the structural unit and presented the first SPH-based simulation of the interaction between a fluid and a composite elastic structure. Chen et al

(2024) used the coupling of the δ -SPH model of the fluid phase (Antuono (2010)) and the TL-SPH model of the elastic solid structure (Belytschko (2000)) to study the role of EHPB and waves.

The currently investigated CFD methods for wave and elastic plate action focus on vertical elastic plates, and there is a lack of validation and research on EHPBs. The meshless methods for EHPB comparison do not consider multiphase flow effects. In this study, we want to reduce the effect of large deformation on the mesh discretization problem by introducing overlapping meshes, and at the same time, we propose a set of CFD-FEM solution methods in combination with the finite element method. The modelling, method validation, and elastic effect study will be discussed in the following.

NUMERICAL METHOD

In this section, a two-way coupled CFD-FEA (Computational Fluid Dynamics and Finite Element Analysis) method is proposed to investigate the dam break problem. The main framework of the coupling strategy will be discussed in this section. The fluid domain is solved by OpenFOAM (Jasak (1996) and Rusche (2002)) with RANS model and VOF method. Calculix, an open-source FEA software, is employed to solve the structure part. The coupling library for partitioned multiphysics simulations, known as preCICE (Chourdakis et al., 2022), is utilized to couple the fluid part and the structure part using a strong implicit way.

Fluid part

The overInterDyMFoam solver with overset method in OpenFOAM ESI v2206 is employed in the fluid part. OpenFOAM uses the PIMPLE algorithm - a combination of Pressure-Implicit with Splitting of Operators (PISO) algorithm and Semi-Implicit Method for Pressure Linked Equations (SIMPLE) algorithm - to decouple velocity and pressure.

The use of incompressible models to study the dam break problem is common as well as stable approach in the current research field. The equations of the RANS method are shown as follows:

$$\nabla \cdot \mathbf{U} = 0 \quad (1)$$

$$\frac{\partial \rho \mathbf{U}}{\partial t} + \nabla \cdot [\rho(\mathbf{U} - \mathbf{U}_g)\mathbf{U}] = -\nabla p_d - \mathbf{g} \cdot \mathbf{x} \nabla \rho + \nabla \cdot (\mu_{eff} \nabla \mathbf{U}) + (\nabla \mathbf{U}) \cdot \nabla \mu_{eff} + \mathbf{f}_\sigma + \mathbf{f}_s \quad (2)$$

In equations (1) and (2) above, \mathbf{U} is the velocity field; \mathbf{U}_g is the grid moving speed; $p_d = p - \rho \mathbf{g} \cdot \mathbf{x}$ is the fluid dynamic pressure; \mathbf{x} is the fluid coordinate position vector; ρ is the density of liquid or gas; \mathbf{g} is the gravitational acceleration vector; $\mu_{eff} = \rho(v + v_t)$ is the effective dynamic viscosity, where v and v_t are called kinematic viscosity and turbulent eddy viscosity, respectively, and the latter is solved by the turbulence model; \mathbf{f}_σ is the surface tension term in the two-phase flow model; and \mathbf{f}_s is the source term applied in the extinction region. $k - \omega$ SST model (Menter et al. (2009)) is used to solve the turbulent eddy viscosity v_t

When it comes to the free surface capture, the VOF method (Berberović et al. (2009)) with artificial compression is used to solve the problem. The transport equation of the phase fraction is equation (3)

$$\frac{\partial \alpha}{\partial t} + \nabla \cdot [(\mathbf{U} - \mathbf{U}_g)\alpha] + \nabla \cdot [\mathbf{U}_r(1 - \alpha)\alpha] = 0 \quad (3)$$

where α is the phase fraction between 0 and 1. Different values of α represents the following meanings in equation (4):

$$\begin{cases} \alpha = 0 & \text{air} \\ \alpha = 1 & \text{water} \\ 0 < \alpha < 1 & \text{interface} \end{cases} \quad (4)$$

The open-source library waves2Foam (Jensen et al. (2014)), based on the relaxation zone method, was used to simulate wave generation and absorption. The theoretical and numerical solutions are weighted and combined within the relaxation zones set up in the viscous flow inlet and outlet regions, using a relaxation function as shown in equations (5) and (6)

$$\phi = \omega_R \phi_{computed} + (1 - \omega_R) \phi_{theory} \quad (5)$$

$$\omega_R = 1 - \frac{\exp(X^{3.5}) - 1}{\exp(1) - 1}, x \in [0,1] \quad (6)$$

ϕ is the fluid velocity or volume fraction; ω_R is the relaxation factor, between 0 and 1; and X is the relative position within the relaxation zone, between 0 and 1. The boundary relaxation factor is 0 in the computational domain, and the boundary relaxation factor of the relaxation zone in the viscous flow computational domain is 1. Waves can be both generated and absorbed in the relaxation zone, where the wave absorption efficiency is sensitive to the length of the relaxation zone. A longer relaxation zone can improve the wave absorption efficiency, but it will increase the number of grids and increase the computational cost, so it is necessary to choose the appropriate length of the relaxation zone.

Structures subjected to slamming loads usually have large vertical motions, and the use of deformed mesh techniques can make calculations impossible due to severe deformation of the mesh. For this reason, the overlapping mesh technique is used: each part of the object is divided into separate meshes, which are independent of each other and are connected by interpolation; the flow field mesh and the object mesh can produce unconstrained displacements and the mesh mass remains unchanged, which ensures the stability of the calculation of the object's large-scale motion. The exchange of flow field information between different meshes in the overlapping mesh is achieved by interpolating values on the overlapping areas of the meshes. The Inverse distance interpolation method is used in overset solver in OpenFOAM ESI V2206. As shown in Fig.1, The red dashed line denotes the active cell, the black realization denotes the contributing cell, and the weight function ω_i is showed in equation (7). The Inverse Distance Interpolation can quickly and easily exchange the physical information of the interpolating unit and the active unit to improve the computational efficiency. Meanwhile, the interpolation accuracy meets the needs of numerical simulation.

$$\omega_i = \frac{1}{|d_i|} / \sum_i^n \frac{1}{|d_i|} \quad (7)$$

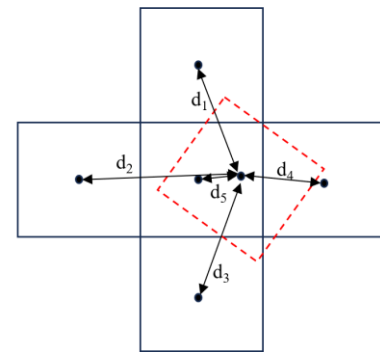


Fig. 1 Inverse distance interpolation method.

where d_i denotes the distance from the center of the contributing cell to the center of the active cell and n denotes the number of contributing cells. The physical quantity field $\phi_{interpolate}$ such as the pressure field p of the active cell can be obtained by interpolating the physical quantity field on the contributing cell, calculated as equation (8)

$$\phi_{interpolate} = \sum_i^n \omega_i \phi_i \quad (8)$$

Structural part

The structural responses of the beam are calculated using Calculix, a free software three-dimensional structural finite element program which makes use of the Abaqus input format. It is possible to use commercial pre-processors. The four-node continuum shell element (S4R) and eight-node brick element with reduced integration solid element (C3D8R) is used to discretize the wedge structure. One end of the beam is fixed to form a cantilever beam structure. The dynamic movement of the wedge is described via displacement field u and the equation is shown in equation (9):

$$M\ddot{u} + C\dot{u} + Ku = q \quad (9)$$

where M, K, C are the structure mass, stiffness and damping $n \times n$ matrix. The damping matrix used Rayleigh damping which is a linear combination of mass and stiffness of the structure. The dynamic equation is solved by generalized alpha method.

Two-way Coupled method

In this paper, the multi-physics field coupling library preCICE is used to couple the above fluid solver with the structure solver to achieve a two-way coupled solver. preCICE is an open-source massively parallel system-based coupling library for partitioned multi-physics field simulations jointly developed by the Technical University of Munich and the University of Stuttgart in Germany using C++. It is powerful enough to be used as a third-party coupling tool to couple OpenFOAM flow field calculations with other open-source FEM solvers such as Calculix (Uekermann et al., 2017, Chourdakis et al., 2023). This approach has been successfully applied to study the fluid-structure interaction problems in water-entry slamming (Xiao et al., 2024) and ship hydroelasticity (Zhang et al., 2025). For coupling solutions, preCICE uses adapter as an interface to interpolate and exchange data directly without modifying the underlying code, just by calling the libpreCICE library in each open-source program.

NUMERICAL SIMULATIONS

Validation of CFD-FEA Method

A benchmark simulation example conducted by Chen et al. (2024) is introduced in this section to investigate wave interaction with an elastic horizontal plate breakwater (EHPB). The numerical flume set up is shown in Fig. 2. The grid is encrypted over a range of wave heights to ensure wave generation. The flume is $4.2L+2.25m$ long. The source zone and wave Absorber zone are both $1.3L$ long. L is the wavelength that varies with the wave period. The depth is $0.5m$. EHPB is set below $0.075m$ the free-surface with fixed-ends on both sides. It is $0.75m$ long and $0.025m$ thick with $0.025m$ fixed-ends on both sides. The density ρ is 1500 kg/m^3 and ν is 0.4 . Point A is in the middle of EHPB to measure the deformation of the structure. To study the reflection coefficient K_r and transmission coefficient K_t . Three wave gauges are set in the flume. G1 and G2 are set at $0.6L$ and $0.35L$ from the left side of EHPB. G3 is

set at $0.7m$ from the right side of EHPB. The reflection coefficient K_r is defined as $K_r = H_r/H$. H_r is the reflected wave height which is estimated with G1 and G2 through two-point method. (Goda, Suzuki (1976)) Transmission coefficient K_t is defined as $K_t = H_3/H$. H is the wave height.

To study the fluid and solid convergence of the fluid mesh. A standard condition with $H=0.04m$, $T=1.2s$ and $L=2.052m$ and the structure Young's modulus $E=3MPa$ is introduced in this section. Three cell size results are introduced which differ from $0.025m$, $0.0125m$ and $0.00625m$ are compared with the theory in Fig. 3. η is the wave height. It could be concluded from the figure that the fluid mesh is monotonic convergence. The medium size of $0.0125m$ is chosen to study the solid mesh convergence. The parameters are shown in table 1. Delta time Δt is $0.005s$.

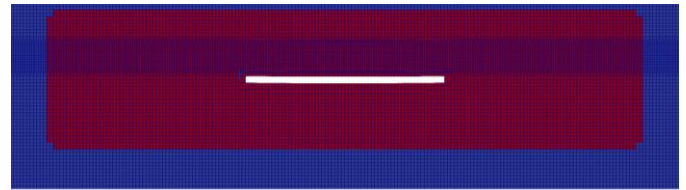
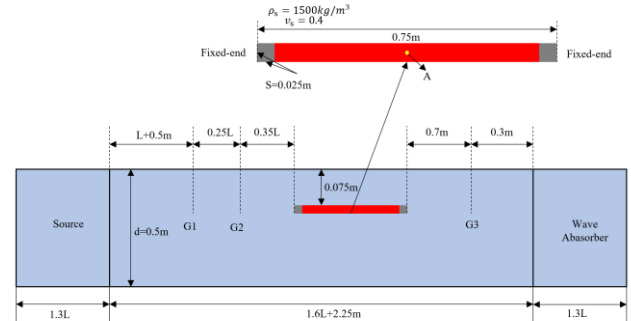


Fig. 2 Numerical flume set up.

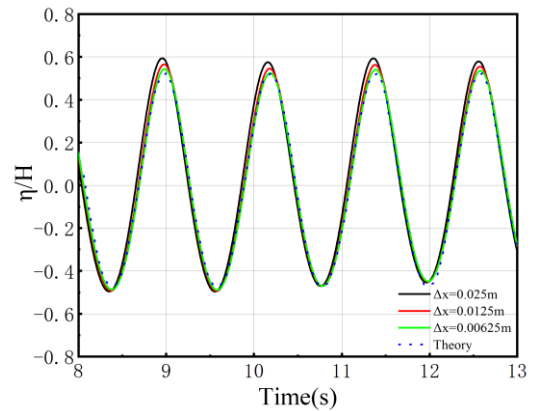


Fig. 3 Comparison of three cell size wave evolution with theory result.

Table 1. Parameter settings of fluid and structure simulations.

Parameter	Value
E	3 MPa
ρ	1500 kg/m^3
ν	0.4
Δt	0.005 s

Three sizes of solid mesh are set to study the solid mesh convergence

which differ from 0.0125m 0.0833m and 0.00625m. The maximum deformation of each size is shown in table 2. The simulation results of the three structural mesh sizes relative difference with the minimum size is smaller than 2.8%. We chose 0.0125 structural grid which is close to the size of the fluid mesh for calculation.

Table 2. Structural deformation results of different cell type.

Cell size	Max top displacement	Relative difference
0.0125m	0.01994 m	2.8%
0.0833m	0.01955 m	0.8%
0.00625m	0.01939 m	/

After the simulation we choose $\Delta x_{fluid} = 0.0125m$ and $\Delta x_{solid} = 0.0125m$ to study wave interaction with EHPB. We investigate 11 wave period and length with $H=0.04m$ which were shown in table 3.

Table 3. Parameters of waves period and length with $H=0.04m$.

T (s)	L (m)
1	1.514
1.1	1.784
1.2	2.052
1.3	2.317
1.4	2.577
1.5	2.834
1.6	3.087
1.7	3.336
1.8	3.583
1.9	3.827
2	4.07

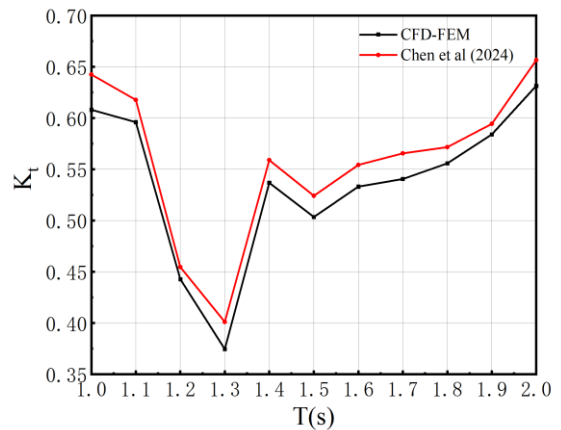
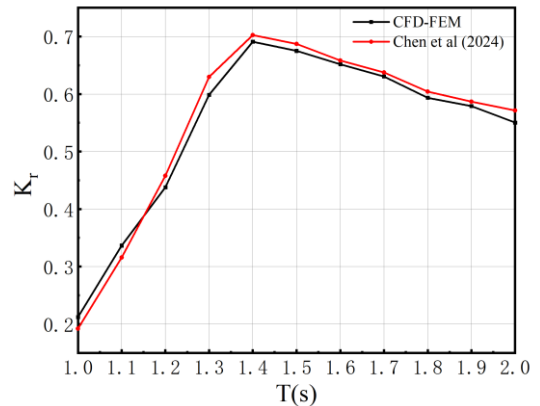
The reflection coefficient K_r , transmission coefficient K_t and The $RAO = \delta_z/H$ of the deformation δ_z at point A is study to validate the CFD-FEM method and the wave generation in Fig. 4. It could be found that the three curves fit well with the trend of the literature results. Meanwhile, from table 4, it can be seen that the maximum error of K_r is 10.3%, the maximum error of K_t is 6.6%, and the maximum error of RAO is 9.7%. The above results prove that the current proposed CFD-FEM method can be used in the study of EHPB.

In this study, the structural deformation response calculations are closer to the literature results. The reflection and transmission coefficients are in large error with the literature results around 1.0s-1.2s, which is correlated with the structural response error. However, it may also be affected by wave dissipation and relaxation zone reflections.

Table 4. Comparison of K_r , K_t RAO between CFD and literature.

T (s)	K_r CFD-FEM	K_r Chen et al (2024)	Error E
1.0	0.2122	0.1923	10.3%
1.1	0.3366	0.3158	6.6%
1.2	0.4378	0.458	4.4%
1.3	0.5986	0.6296	4.9%
1.4	0.6907	0.7023	1.7%
1.5	0.6750	0.687	1.7%
1.6	0.6515	0.6583	1.0%
1.7	0.6303	0.6376	1.1%

1.8	0.5934	0.6042	1.8%
1.9	0.5789	0.5868	1.3%
2.0	0.5404	0.5715	5.4%
T (s)	K_t CFD-FEM	K_t Chen et al (2024)	Error E
1.0	0.6080	0.6424	5.4%
1.1	0.5960	0.6177	3.5%
1.2	0.4428	0.4546	2.6%
1.3	0.3745	0.4011	6.6%
1.4	0.5368	0.5589	4.0%
1.5	0.5035	0.5241	3.9%
1.6	0.5330	0.5542	3.8%
1.7	0.5405	0.5656	4.4%
1.8	0.5558	0.5716	2.8%
1.9	0.5840	0.5943	1.7%
2.0	0.6315	0.6565	3.8%
T (s)	RAO CFD-FEM	RAO Chen et al (2024)	Error E
1.0	0.3486	0.3269	6.6%
1.1	0.3716	0.3388	9.7%
1.2	0.4185	0.3860	8.4%
1.3	0.6757	0.6970	3.1%
1.4	0.7340	0.7256	1.2%
1.5	0.5428	0.5209	4.2%
1.6	0.5263	0.5136	2.5%
1.7	0.4728	0.4731	0.1%
1.8	0.5002	0.5083	1.6%
1.9	0.6304	0.6552	3.8%
2.0	0.6933	0.7216	3.9%



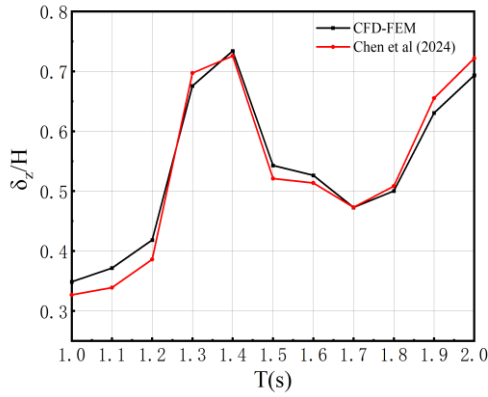


Fig. 4 Comparison of $K_r = H_r/H$, $K_t = H_3/H$ and $RAO = \delta_z/H$ at point A with literature results.

Effects of elasticity

In this section the effects of elasticity are studied. Rigid horizontal plate breakwater (RHPB, $E=3MPa$) is set up to compare the reflection coefficient K_r and transmission coefficient K_t with Elastic horizontal plate breakwater (EHPB). Fig 5 shows the comparison of K_r between EHPB and RHPB. When $T=1.1s-1.4s$ EHPB's K_r is larger than RHPB while RHPB's K_r is larger than EHPB. The K_r of EHPB is larger in the shorter wave and RHPB's is larger in the longer wave, except for $T=1.0s$. Fig. 6 is the comparison of K_t between EHPB and RHPB. RHPB is larger than EHPB when $T < 1.6s$ while RHPB behave better than EHPB when $T > 1.6s$.

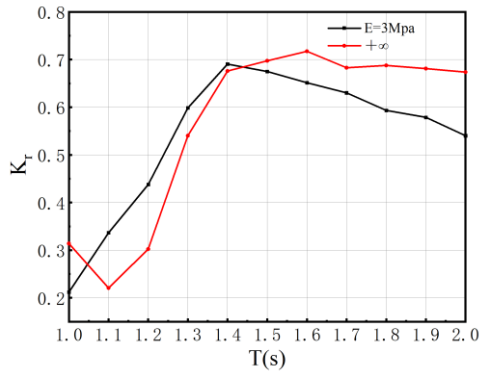


Fig. 5 Comparison of $K_r = H_r/H$ between EHPB and RHPB.

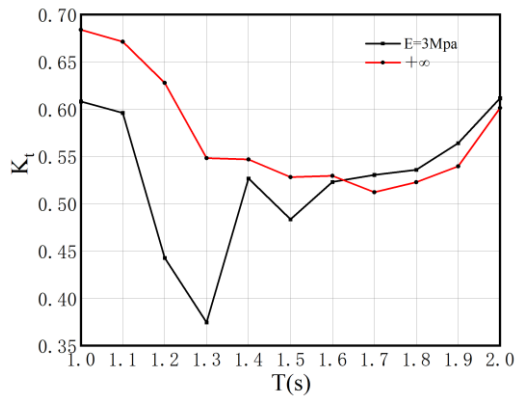
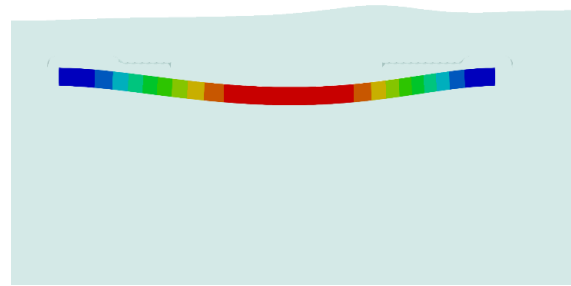


Fig. 6 Comparison of $K_t = H_3/H$ between EHPB and RHPB.

It could be concluded that the effects of elasticity may be not obvious at the longer wave at $H=0.04m$. When $T < 1.6s$ which we could define these waves short wave EHPB's performance is better. $T=1.2s$ is chosen to investigate the interaction with waves between EHPB and RHPB.

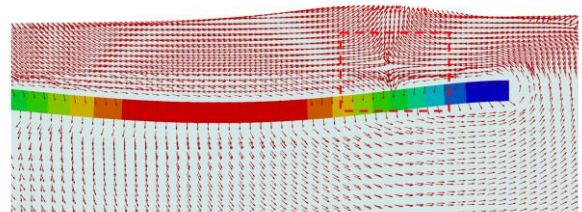


EHPB ($E=3MPa$)

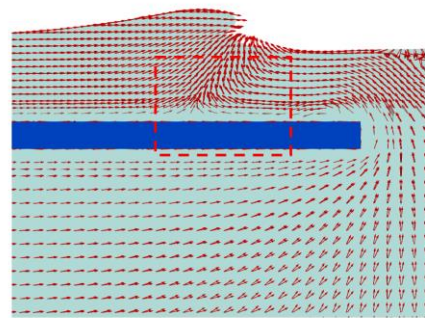


RHPB

Fig. 7. Wave evolution at $t=0.5T$, $T=1.2s$, $H=0.04m$.



EHPB ($E=3MPa$)



RHPB

Fig. 8. Velocity field at $t=0.5T$, $T=1.2s$, $H=0.04m$.

Fig. 7 is the wave evolution at $t=0.5$ of case $T=1.2s$. The deformation of the EHPB resulted in a calmer wave surface. In the case of RHPB installations, breakage will occur if the wave steepness is too large to maintain the wave surface. We further investigated the flow velocity distribution inside the flow field as shown in Fig. 8. The deformation of the EHPB resulting in the sinking of the lower body of water on the upper surface of the breaker will have consumed some of the energy. The above phenomenon prevents the wave breaking phenomenon from occurring.

CONCLUSIONS

This paper proposed a two-way coupled CFD-FEM program is applied to numerically simulate wave interaction with elastic horizontal plate breakwaters. Overset method and waves2Foam open-source library was used to hydrodynamics and wave generation. Results of $T=1.2s$, $H=0.04m$ regular wave interaction with $E=3MPa$ EHPB is compared with literature results (Chen et al. (2024)). The maximum error of reflection coefficient K_r is 10.3%, the maximum error of transmission coefficient K_t is 6.6%, and the maximum error of RAO of the deformation δ_z at point A is 9.7%. The above results prove that the current proposed CFD-FEM method can be used in the study of EHPB.

Effects of elasticity is investigated in this work. EHPB is compare with RHPB. The comparison of K_r and K_t shows that in the regular wave $H=0.04m$. EHPB behave better than RHPB in shorter wave ($T \leq 1.6s$), while RHPB is better in longer wave ($T > 1.6s$). The deformation of breakwater can prevent the generation of breaking waves and make the wave surface smoother.

Further work could be concentrated on different wave height, materials and even irregular wave.

ACKNOWLEDGEMENTS

This work is supported by the National Natural Science Foundation of China (52131102), to which the authors are most grateful.

REFERENCES

- Antuono M, Colagrossi A, Marrone S, Molteni D. 2010. Free-surface flows solved by means of SPH schemes with numerical diffusive terms. *Comput Phys Commun*; 181:532–49.
- Ashok R, Gunasundari C, Manam S. 2020. Explicit solutions of the scattering problems involving vertical flexible porous structures. *J Fluid Struct*; 99:103149.
- Attili T, Heller V, Triantafyllou T. 2023. Wave impact on rigid and flexible plates. *Coast Eng*; 182:104302.
- Belytschko T, Guo Y, Liu W, Xiao S. 2000. A unified stability analysis of meshless particle methods. *Int J Numer Methods Eng*; 48:1359–400.
- Brossard J, Perret G, Blonce L, Diedhiou A. 2009. Higher harmonics induced by a submerged horizontal plate and a submerged rectangular step in a wave flume. *Coast Eng*; 56:11 – 22.
- Berberović, E., van Hinsberg, N., Jakirlić, S., Roisman, I., Tropea, C., 2009. Drop impact onto a liquid layer of finite thickness: dynamics of the cavity evolution. *Phys. Rev. E* 79 (3), 36306.
- Cardiff P, Karać A, Jaeger P, Jasak H, Nagy J, Ivanković A, et al. 2018. An open-source finite volume toolbox for solid mechanics and fluid-solid interaction simulations. *ArXiv Prepr*.
- Chen Y.K, Meringolo D.D, Liu Y, et al. 2024. SPH numerical model of wave interaction with elastic thin structures and its application to elastic horizontal plate breakwater. *Marine Struct.*, 93: 103531.
- Chourdakis G., Davis K., Rodenberg B, et al., 2022. preCICE v2: A sustainable and user-friendly coupling library. *Open Res Eur.*, 2:51.
- Chourdakis G., Schneider D and Uekermann B, 2023. OpenFOAM-preCICE: Coupling OpenFOAM with External Solvers for Multi-Physics Simulations. *OpenFOAM@ Journal*, 3:1-25.
- Goda Y, Suzuki Y. 1976. Estimation of incident and reflected waves in random wave experiments. *Coastal Engin.* 1:47.
- Greene T, Heins A. 1953. Water waves over a channel of infinite depth. *Q Appl Math*; 11:201–14.
- Jasak, H.,1996. Error Analysis and Estimation for the Finite Volume Method with Applications to Fluid Flows. Imperial College, London, UK (Ph.D. thesis).
- Heins A. 1950. Water waves over a channel of finite depth with a submerged plane barrier. *Can J Math*: 210–22.
- Hu Z, Huang L, Li Y. 2023. Fully-coupled hydroelastic modeling of a deformable wall in waves. *Coast Eng*; 179:104245.
- Ijima T, Ozaki S, Eguchi Y, Kobayashi A. 1970. Breakwater and quay well by horizontal plates. In: *Proceedings of the 12th coastal engineering conference on ASCE*; p. 1537 – 56.
- Jensen B, Jacobsen N.G, Christensen E.D, 2014. Investigations on the porous media equations and resistance coefficients for coastal structures. *Coastal Engin.* 84:56-72.
- Khayyer A, Shimizu Y, Gotoh H, Nagashima K. 2021. A coupled incompressible SPH-Hamiltonian SPH solver for hydroelastic FSI corresponding to composite structures. *Applied Mathematical Modeling*; 94:242–71.
- Lee J, Chen C. 2010. Wave interaction with hinged flexible breakwater. *J Hydraul Res*; 28:283–97.
- Liao K, Hu C. 2013. A coupled FDM–FEM method for free surface flow interaction with thin elastic plate. *J Mar Sci Technol*; 18:1–11.
- Menter F R, 2009. Review of the shear-stress transport turbulence model experience from an industrial perspective. *Int. J. Comput. Fluid Dyn.* 23 (4), 305–316.
- Phadke A, Cheung K. 1999. Response of bottom-mounted fluid-filled membrane in gravity waves. *J Waterw Port, Coast Ocean Eng*; 125:294–303.
- Qi P, Hou Y. 2003. Numerical wave flume study on wave motion around submerged plates. *China Ocean Eng* 2003; 17:397 – 406.
- Rusche H, 2002. *Computational Fluid Dynamics of Dispersed Two-phase Flows at High Phase Fractions*. Imperial College, London, UK (Ph.D. thesis).
- Uekermann B, Bungartz H-J, Yau LC, et al., 2017. Official preCICE Adapters for Standard Open-Source Solvers. *Proceedings of the 7th GACM Colloquium on Computational Mechanics for Young Scientists from Academia*. Stuttgart, Germany Oct 10-13.
- Xiao J, Liu J, Han B, Wan D and Wang J, 2024. A two-way coupled fluid–structure interaction method for predicting the slamming loads and structural responses on a stiffened wedge. *Phys. Fluids*, 36, 077123.
- Zhang W, Wang J, Guo H, Liu Y and Wan D, 2025, Numerical investigations of ship hydroelasticity of a 20,000 TEU containership based on CFD-MBD method. *Ocean Eng.*, 317, 120061.